Modification of Turbulent Flow Using Distributed Transpiration

Maurizio Quadrio * J.M. Floryan ** Paolo Luchini ***

Abstract

The long-term objective of this investigation is the development of techniques for re-arrangement and control of turbulent flows by using a suitably roughened wall. As a preliminary step towards this goal, we describe the analysis of the turbulent flow in a plane channel modified by a sinusoidal distribution of suction and blowing at the wall with zero net mass flux. The tool by which the whole investigation is carried out is the Direct Numerical Simulation of the incompressible Navier–Stokes equations. The fundamental result of this preliminary study is that the transpiration wavelength has a dramatic effect on the modification induced on the turbulent flow by the wall transpiration. Large wavelengths produce very high increases in the frictional drag, whereas smaller wavelengths can lead to a friction decrease of up to 4%–5%.

Résumé

L'objectif à long terme de cette recherche consiste à élaborer des techniques relatives au réarrangement et au contrôle des écoulements turbulents à l'aide de parois pourvues d'aspérités. À titre d'étape préliminaire vers cet objectif, nous décrivons dans le présent document l'analyse de l'écoulement turbulent dans un canal lisse modifié par une distribution sinusoïdale d'aspiration/de soufflage à la paroi avec un flux de masse nette nul. L'outil utilisé dans cette recherche est la simulation numérique directe des équations de Navier–Stokes pour un fluide incompressible. Le résultat principal de cette étude préliminaire est que la longueur d'onde de transpiration a un effet notable sur la modification apportée à l'écoulement turbulent par la

continued on page 62

* Department of Aerospace Engineering, Politecnico di Milano, Campus Bovisa via La Masa 34, Milan 20156, Italy.
E-mail: maurizio.quadrio@polimi.it

** Department of Mechanical Materials Engineering, The University of Western Ontario, London, ON N6A 5B9, Canada.

*** Department of Mechanical Engineering, University of Salerno, Italy.

Received 8 July 2003.

Introduction and Motivation

The use of distributed transpiration through a wall with a fluid flowing over it in the turbulent regime is a typical application where one tries to affect and control the turbulence properties via a suitable control strategy applied at the wall. The technological relevance and the scientific interest of the studies aimed at controlling turbulent flows are today widely recognized (Bewley, 2001). A detailed knowledge of the turbulence-producing cycle taking place in the near-wall region of a wall-bounded shear flow is a preliminary step towards the ability of controlling the flow itself. The control is typically focused towards one of the two classical objectives of reducing the friction drag and increasing the turbulent mixing and heat transfer. Control techniques are classified as either active techniques (when relying on some external energy input), and (or) as closed-loop techniques (when based on non-trival feedback control laws).

Among the inherently simpler passive open-loop strategies, one that has received some attention to date is the use of non-planar surfaces. One such example is the use of riblets (Bechert et al., 1997), i.e., small-scale V-grooves aligned in the streamwise direction, which can produce up to 8%–10% reductions in turbulent friction drag. As recently underlined by Jiménez (2004), the analysis of other wall shapes (besides riblets) is certainly worth further consideration. While it is well known that the shape of the roughness profile may directly affect the turbulent flow, there is no indication to date of a particular roughness shape other than riblets that reduces drag, and at the same time there is no reason to exclude that such shapes may exist. Considering in particular the sinusoidal shape, i.e., a sinusoidal variation of the wall geometry with the streamwise coordinate, there are indeed quite a few papers related to turbulent flow over a wavy wall, but a systematic analysis of the whole parameter set for the corrugation has never been carried out. Hence, the effects of such a roughness shape are to date not fully known.

Besides its potential for flow control, the turbulent flow over a wavy wall is interesting per se, in particular for the interaction of the streamwise, alternately convex–concave curvature with the turbulent flow. In the recent literature, evidence of large-scale streamwise Taylor–Görtler-type vortices is found in the experimental analysis by Gschwind et al. (1995). In their wavy channel, however, the ratio between wave amplitude and channel height is so large as to make it essentially a quasi-planar flow problem with mild streamwise curvature. Some

© 2005 CASI

suite de la page 61

transpiration de paroi. Les grandes longueurs d'onde génèrent des augmentations importantes de la traînée de frottement, alors que les longueurs d'onde moins élevées peuvent donner lieu à une diminution du frottement allant jusqu'à 4 % à 5 %.

large-scale streamwise vortical structures, in the range of parameters where curvature effects are comparable to those considered in the present work, have been found by Gong et al. (1996) and recently confirmed by Günther and Rudolph von Rohr (2003). In this last experiment, carried out with a wavelength λ of the corrugation equal to the full height $2h$ of the channel, and with a peak-to-peak distance of 0.1λ Günther and Rudolph von Rohr (2003) found with a Proper Orthogonal Decomposition of the velocity fluctuations that the dominant eigenmodes possess a characteristic spanwise scale of $3h$, and are consistent with the existence of streamwise-oriented large-scale vortical structures. They state that the only parameter that characterizes the flow, besides the Reynolds number based on the channel height, is the ratio between roughness wavelength and peak-to-peak amplitude, thus neglecting the importance of the value λ^+ of the wavelength expressed in wall units (in this paper, quantities indicated with a + superscript are made non-dimensional using the friction velocity and the fluid viscosity). The very presence of longitudinal vortices is still an issue under discussion. It can be explained with a Craik–Leibovich type-2 (CL2) instability, as described in Phillips et al. (1996), but can be explained also by centrifugal effects due to a Görtler-type instability. The last mechanism cannot be ruled out at the present state of our knowledge.

The turbulent boundary layer over a wavy wall has been studied by Hanratty and co-workers, for many years, at the University of Illinois, both with experiments and Direct Numerical Simulation (DNS). For example, Cherukat et al. (1998) exhaustively investigated with DNS the turbulent flow over a wavy wall with wavelength $\lambda = 2h$, replicating a similar experimental analysis described in Hudson et al. (1996). Another DNS-based numerical study is reported in the paper by De Angelis et al. (1997): $\lambda = 1.04h$ and $\lambda = 2.09h$ were considered. It is easily seen that almost all analyses available to date considered only wavelengths comparable to the channel half-width.

The flow over a wavy wall has been extensively studied in the laminar flow regime. Floryan (2002) and Cabal et al. (2002) found with a linear stability analysis that a two-dimensional, sinusoidal waviness of the wall described in terms of a single Fourier mode in the streamwise direction can affect the stability properties of the laminar flow in a significant way. They found a range of corrugation wavelengths, bounded from above and from below, where a new type of instability, due to centrifugal effects, determines the appearance of streamwise vortices, arranged in the spanwise direction with a preferred wavelength. This conclusion has been reached for both Couette and Poiseuille flows. It is not clear however how these results (and the results from the CL2 instability mechanism) apply to the turbulent flow in a wavy channel.

In this preliminary stage of the research, we study through a number of numerical experiments, based on DNS, the properties of the turbulent channel flow over a simulated two-dimensional distributed surface roughness, obtained through a sinusoidal distribution of blowing and suction velocities in the wall-normal direction, with zero net mass flux. The equivalence between a wavy wall and a sinusoidal distribution of suction velocity at a planar wall still has to be proven; nevertheless, Floryan (1997) found that the mechanisms governing the transition process are qualitatively similar. In the literature, there is only one paper dealing with a similar flow configuration, i.e., the paper by Jiménez et al. (2001). These authors investigated numerically the effect of a wall transpiration proportional to the local, instantaneous value of the pressure fluctuations, and found that the skin friction increases up to 40%. This increase is reportedly due to a large-scale reorganization of the flow: the transpiration adjusts itself into a two-dimensional, spanwise-coherent pattern, producing large coherent rolls of spanwise vorticity. A subset of the numerical experiments described by Jiménez et al. (2001) was devoted to the study of the same flow configuration that we are considering in this paper, but the wavelength was kept fixed at the value suggested by the naturally occurring rolls in the passive porosity case.

The aim of the present paper is to complete the assessment of the effects of sinusoidal transpiration on turbulent flow, investigating in more detail how they are functions of its two parameters (amplitude and wavelength). The structure of the paper is as follows. First a brief overview of the available techniques for the control of turbulent flow will be given; then the numerical method and the computer code used for the simulations will be described, and the discretization and the parameters used in the simulations to characterize the transpiration will be illustrated. We will then report results concerning the modification of the mean friction induced by the transpiration: turbulent statistics, first averaged over the whole channel and then as a function of the streamwise position over the suction distribution, will be eventually used to illustrate the modification of the turbulent flow under the action of the transpiration.

Control of Turbulent Flows

In recent years, the improvement in our knowledge of turbulence, and the very possibility offered by micro-electro-mechanical systems (MEMS) to deploy a fine-scale distribution of sensors and actuators on a large surface area (Ho and Tai, 1998) has boosted the number of studies related to turbulence control and drag reduction. Following the use of riblets and the injection (in liquid flows) of long-chain polymeric molecules, several attempts to control a turbulent wall flow by employing a number of different techniques are reported in the recent

© 2005 CASI

literature. Most of them are in the proof-of-principle stage, and the tool used for developing and testing the control strategies is most often the DNS of the incompressible Navier–Stokes equations. Thanks to this research tool, different ideas can be tested in a cost-effective manner, and even unphysical simulations can be carried out, with the aim of gaining additional insight into the real physics of the flow (Moin and Mahesh, 1998).

Recently developed control techniques span a range from the use of spanwise oscillation of the wall (Jung et al., 1992; Quadrio and Ricco, 2004), to the use of an oscillating Lorentz force (Berger et al., 2000) or a spanwise travelling wave (Du et al., 2002). All these techniques are *open-loop*, since they do not require feedback in the control law. Other, more complex *closed-loop* control strategies can be devised where a feedback is exploited in the control law. We mention in this category the so-called opposition control through a distributed array of sensors (in the interior of the channel) and actuators (local, instantaneous blowing and suction at the wall), introduced by Choi et al. (1994), and the wall vorticity flux control by Koumoutsakos (1999), which uses the same type of actuators but relies only on information available at the wall. An additional class of active, closed-loop control systems is growing, which can be broadly classified as optimal (or suboptimal) controls. They employ concepts from control theory (Joshy et al., 1997), and in particular one promising approach exploits the power of adjoint operators, computing the Fréchet derivative of a cost function to optimize friction drag. Some examples are described in Lee et al. (1998), Bewley et al. (2001), and Luchini and Quadrio (2002).

It is clear however that passive, open-loop techniques (like riblets) are best suited for practical implementations: they do not require sensors or actuators and control law, nor do they depend on external energy input to function. This is why we focus in the following on relatively simple shape modifications of a planar rigid surface, and, in particular, on the modifications modeling through distributed transpiration.

The Numerical Method

The DNS code used in this paper is a parallel solver of the Navier–Stokes equations for an incompressible fluid, used to compute the turbulent flow in an indefinite plane channel. The geometry and reference system are sketched in **Figure 1**.

A brief description of the numerical method can be found in Quadrio and Luchini (2001) and Luchini and Quadrio (2005). The code is based on a mixed discretization: Fourier modes are used for the wall-parallel directions, and high-order finite differences in the wall-normal direction. Finite differences are produced from fourth-order accurate, compact schemes acting on a five-point computational molecule in a variable-spacing mesh. Periodic boundary conditions, implied by the Fourier expansions, are used in the streamwise and spanwise directions: it is well known, starting from Kim et al. (1987), that periodic conditions can be employed for the homogeneous directions,

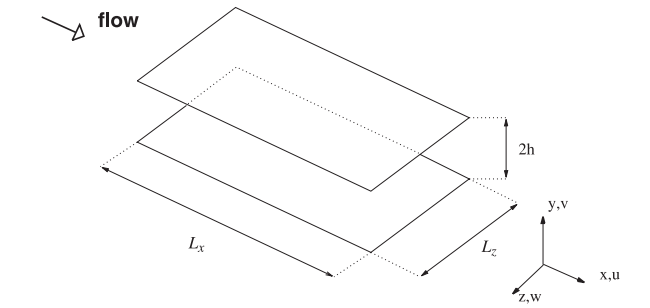

Figure 1. Sketch of the computational domain and reference system.

provided the length and width of the computational domain are chosen accordingly. At the wall, the no-slip conditions are enforced. In this work, the no-penetration condition for the wall-normal component is replaced by the transpiration condition (1), as discussed in the following.

The Navier–Stokes equations are formulated, following a procedure described in Kim et al. (1987), in terms of a scalar equation for the wall-normal component of velocity, and a scalar equation for the wall-normal component of vorticity, thus achieving the highest computational efficiency when a Fourier discretization is adopted for the homogeneous directions. The non-linear terms of the equations are computed with a pseudo-spectral approach, transforming the flow variables from Fourier space into physical space before computing the products of the velocity components, and taking advantage of computationally efficient Fast-Fourier-Transform algorithms. The removal of the aliasing error in the homogeneous directions is performed exactly by expanding the number of Fourier modes by a factor of at least 3/2 before going from the Fourier space into the physical space, to avoid the introduction of spurious energy from the high-frequency into the low-frequency modes during the calculations.

The advancement in time of the solution is realized by a commonly used partially implicit approach: non-linear terms are advanced with an explicit scheme (a low-storage, three-substeps, third-order Runge–Kutta scheme), and linear terms are advanced with an implicit method (a second-order Crank–Nicolson scheme) to overcome the stability limitations due to the viscous terms.

The code takes advantage of shared-memory computing systems, and can be run in parallel on a set of distributed-memory machines (nodes). Thanks to the use of finite differences for the discretization of the normal direction, the parallel algorithm requires no inter-node communication as far as the computation of the explicit convective part is concerned. When data are stored in wall-parallel slices, Fourier transforms are in fact executed in wall-parallel planes. The evaluation of wall-normal derivatives can be done without communication as well, at the expense of duplicating in each machine the four boundary planes shared with the two neighboring nodes. Only the numerical solution of the linear systems arising from the discretization of the implicit part requires some communication, but the impact of the communication time on the overall

© 2005 CASI

computing time decreases when the problem size increases, and calculations never happen to be communication-bound. Further details regarding the communications strategy can be found in Luchini and Quadrio (2005).

Computational Parameters

The simulations have been carried out for a value of the Reynolds number, based on h, half the channel height, and U_P, the centerline velocity of a laminar Poiseuille flow with the same flow rate, of $Re_P = 4250$. This corresponds to a value of the Reynolds number based on the friction velocity of $\mathrm{Re}_\tau = 180$; the centerline velocity is $U_c = 0.78U_P$. In the simulations the flow rate is kept fixed at a value which is 4/3 in these units. The computational domain has a streamwise length of $L_x = 2.66\pi h$ and a spanwise width of $L_z = 2\pi h$. 129 × 129 Fourier modes are used to expand the flow variables in the homogeneous directions, so that the spatial resolution is $\Delta x^+ = 11.7$ and $\Delta z^+ = 8.8$. In the wall-normal direction 129 collocation points are used, with a non- uniform spacing from $\Delta y^+ = 0.75$ near the wall to $\Delta y^+ = 4.8$ at the channel centreline. This spatial resolution is in line with many previous computational studies. In particular, the wall-normal resolution is similar to the one typically used in DNS of turbulent wall flows when finite-difference methods are used for the wall-normal direction: indeed Jiménez et al. (2001) use a similar mesh size for a similar problem. To put things into perspective, the Kolmogorov dissipative lengthscale at the wall is around 2 wall units (see, for example, Marati et al., 2004). For increasing time accuracy, the time step for the temporal integration is set at $\Delta t^+ \approx 0.2$, which is lower than the stability limit of the time integration scheme.

The wall transpiration has been accounted for through the wall boundary condition for the wall-normal velocity component v

$$v(x, y = \pm h, z, t) = A\cos(\alpha_s x) \tag{1}$$

where A is the maximum amplitude of the transpiration distribution, and α_s is the transpiration wave number. The blowing and suction distribution has a zero net mass flux over the entire wall, is stationary in time, constant across the spanwise direction and has a sinusoidal variation along the streamwise coordinate, with a wavelength $\lambda_s = 2\pi / \alpha_s$. The wavenumber α_s is always chosen as an integer multiple of the base wavenumber $\alpha_0 = 2\pi/L_x$.

The simulations were started from a fully developed turbulent flow field computed with a previous simulation with transpiration turned off, and various combinations of A and α_s have been used. Most of the simulations have been run for a total integration time of $500h/U_P$; the time evolution of selected quantities, notably the two components of the space-averaged friction over the two walls has been recorded. When turbulence statistics are computed, flow fields are stored on a disk during the calculations for later post processing: a complete flow field is written to disk every $25h/U_P$, so that we typically average over 20 well-separated flow fields. In addition, data from the two walls are averaged together to double the statistical sample.

The simulations described in this paper have been performed using a cluster of Itanium2 computers, available at the Shared Hierarchical Academic Research Computing Network (SHARCNET), Ontario, Canada. In particular each of the 26 computational cases listed in the following has been run by using 4 computing nodes, equipped with two CPU each, and required a total wall-clock time of approximately 20 h.

Initial Choice of the Suction Parameters

We start our analysis from a laminar calculation, similar to those described in Cabal et al. (2002) and Floryan (2002), but using the turbulent mean velocity profile as the base flow. A disturbance in the form of a sinusoidal, two-dimensional blowing and suction distribution of wavelength $\lambda = 2\pi / \alpha_s$ and maximum intensity A is applied at the two walls of a plane channel flow, and the growth rate of the most unstable disturbance is computed for a value of the Reynolds number of $Re_c = 3300$ (based on the channel half-width and the maximum centerline velocity). The base flow coincides with the turbulent longitudinal mean velocity profile previously computed with a DNS at the same Reynolds number, and corresponds to $\mathrm{Re}_\tau = 180$ and $Re_P = 4250$.

Disturbances to the base flow have the form

$$v(x, y, z, t) = \sum_{m=-\infty}^{+\infty} V_m(y) \exp[i(m\alpha_s x + \mu z - \sigma t)]$$

where v is one component of the disturbance vector, $V(y)$ is a corresponding function of the wall-normal coordinate only, z is the spanwise coordinate, and μ accounts for the spanwise periodicity of the streamwise vortices. σ is a purely imaginary number, and describes the growth ($\Im(\sigma) > 0$) or the decay ($\Im(\sigma) < 0$) of the perturbations.

A typical result is illustrated in **Figure 2** for a suction amplitude of $A = 0.004$: the neutral curve $\sigma = 0$ encloses a region where σ is positive. This defines a range of suction wave numbers α_s where centrifugal instability is active, and a corresponding range of spanwise wave numbers. The most amplified streamwise vortex occurs in this particular case for $\alpha_s h = 1.8$ and has a typical spanwise wave number of $\beta h = 2 – 2.5$.

Such results give us an initial guess for the range of interesting suction wave numbers, even if we expected only a qualitative guidance.

Mean Friction

Table 1 reports the time-averaged value of the friction coefficient C_f, defined as

$$C_f = 2\tau_x/\rho U_b^2$$

© 2005 CASI

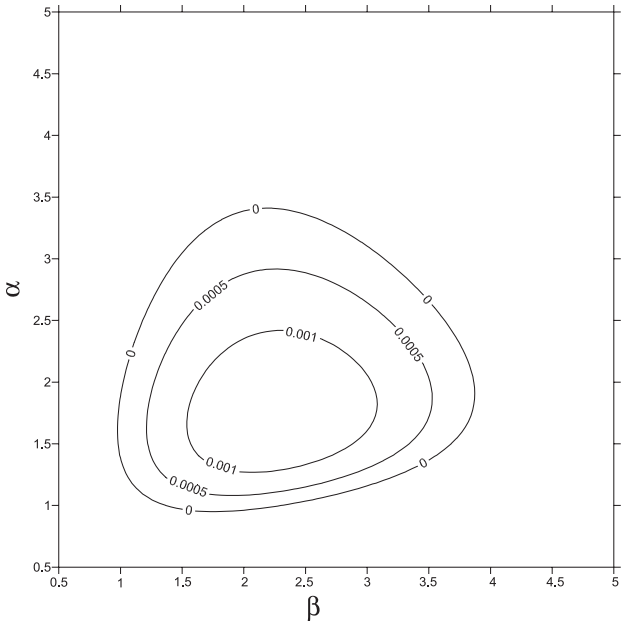

Figure 2. Amplification rate $\Im(\sigma)$ of disturbances in the form of streamwise vortices as a function of the suction wavenumber α_s and the vortex wavenumber β, with Re = 3300 and A = 0.004.

where τ_x is the streamwise component of the shear stress at the wall, and U_b is the bulk velocity of the flow. τ_x is evaluated through the wall-normal derivative of the mean velocity profile at the wall. There is no other contribution to C_f, since the streamwise derivative of the wall-normal velocity component has zero spatial mean. The computed value of $C_f = 8.22 \times 10^{-3}$ in the case without transpiration compares very well with the value obtained by Kim et al. (1987) in the DNS of a turbulent channel flow over an impermeable wall at the same Reynolds number: the difference is only 0.4%.

Figure 3 plots the friction coefficient as a function of the transpiration intensity A, with wave number fixed at $\alpha_s h = 1.5$. The friction is observed to increase with A, and even with modest intensities ($A/U_P = 0.04$ corresponds to $A^+ \approx 0.9$) the increase in C_f is almost three-fold. A threshold of minimum A/U_P appears to be required for the transpiration to affect the turbulent flow.

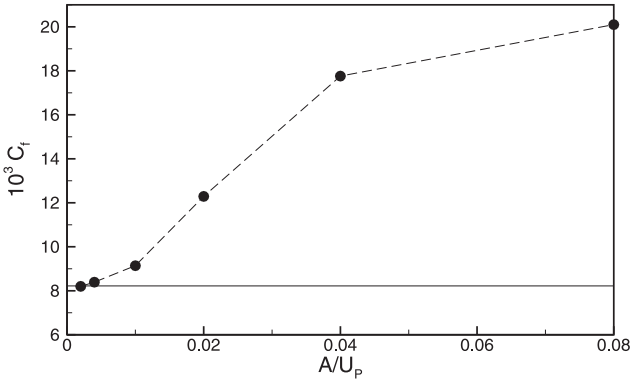

Figure 3. Behavior of the friction coefficient C_f as a function of the maximum intensity of the wall transpiration, for $\alpha_s h$ = 1.5. The horizontal line is the case with A = 0.

Figure 4 shows the changes of C_f versus the transpiration wavelength, for fixed amplitude $A/U_P = 0.02$. The wavelength is expressed in wall units. The points at largest wavelength should be considered with some care, since the wavelength in this case equals the length of the computational domain, and a subharmonic behaviour cannot be ruled our a priori. No evidence for such a behaviour has been however found either in the laminar case, or in the turbulent case for shorter transpiration wavelengths. For shorter wavelenghts, the most important information from this plot shows that, as long as $\lambda^+ <$ 350–400, the friction coefficient goes below the reference value, i.e., the turbulent flow experiences a small decrease of the frictional drag. The maximum measured drag reduction with $A = 0.02U_P$ is 3.8% at $\lambda^+ = 250$. A similar trend can be observed at different values of the transpiration amplitude.

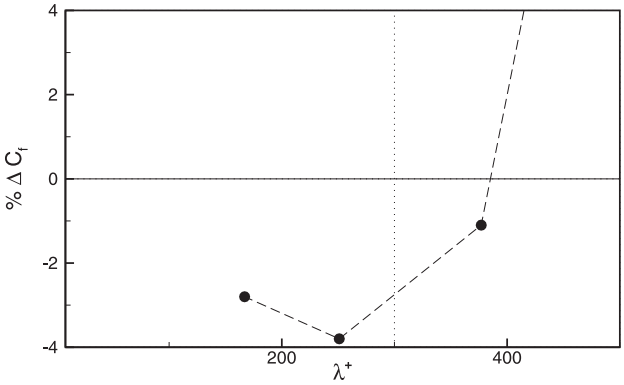

Figure 4. Behavior of the percentage change in friction coefficient as a function of the transpiration wavelength $\lambda^+ = \lambda u_\tau / \nu$ expressed in wall units, for A/U_P = 0.02.

Many more measurement points are clearly needed to fully describe the changes of C_f when the transpiration wavelength is varied. In this preliminary study, however, we limit ourselves to making sure that, regardless of its numerical value, the measured drag reduction is a real phenomenon and not an artifact of numerical errors, poor spatio-temporal resolution, etc. The very good agreement of the computed C_f with the reference value given by Kim et al. (1987) assesses the quality of the simulation in the impermeable-wall case. To quantify the reliability of the C_f measurements in the simulations over the transpirating wall, a few numerical experiments have been repeated with significantly improved spatio-temporal resolution. In particular, the time step size has been halved, the time integration interval has been enlarged to $800h/U_P$, and the number of Fourier modes and wall-normal points has been doubled. This resulted in simulations with 256^3 computational size. The previously mentioned case with $A = 0.02U_P$ and $\lambda^+ =$ 250 has given essentially equivalent results, with $C_f = 7.98 \times 10^{-3}$ and an error in the percentage drag reduction of 0.9% only. Even though this is a significant portion of the whole drag reduction, it permits us to claim that in an interval of

© 2005 CASI

wavelengths centered around $\lambda^+ = 300$ a noticeable drag reduction occurs, larger than the statistical uncertainty of the data. The same trend can indeed be observed at different values of A/U_P, and thus can hardly be considered as the random effect of discretization errors alone. Moreover, we have computed even larger drag reductions by further increasing A, but we have also found via resolution studies that the numerical errors increase further at larger amplitudes, so that larger resolutions are probably needed for a reliable measurement of C_f with larger values of A. The maximum drag reduction reliably measured in these preliminary experiments is 4.4% with $A = 0.03U_P$ and $\alpha_s h = 4.5$.

There is, to our knowledge, no previous available data for friction measurements with distributed non-uniform, sinusoidal suction in a turbulent flow, with the exception of those reported by Jiménez et al. (2001) that are taken at different parameter values and cannot hence be directly compared with the present results. Even in the qualitatively similar flow over a wavy wall, the roughness wavelength has never been varied in a systematic way, as mentioned in the Introduction. In this case, when the wall is not flat the drag budget becomes more complex, since additional terms arise (form drag), so that the overall drag may increase (De Angelis et al., 1997).

The present results are important, since they show that the wavelength of the roughness (or at least of the suction distribution) is a very important parameter of the flow. This is a reasonable finding. The effect of the modulation of the turbulent flow by sinusoidal transpiration on friction must be mediated by its interaction with the near-wall turbulent structures, which are typical of the near-wall region (Robinson, 1991), and are ultimately responsible for the turbulent friction drag. Hence, it is reasonable to expect that the nature of this interaction does depend on the ratio between the wavelength of the waves and the streamwise extension of some typical near-wall structures.

From **Figure 4** an abrupt change of the response of the flow to the distributed transpiration can be noticed around 400 viscous lengths. This is a typical length scale in near-wall turbulence. For example, Jiménez and Moin (1991) in their Minimum Channel DNS determined the minimal extent of the computational domain that is needed to sustain the turbulence cycle, speculating that they correspond to the minimal length scales that are relevant to a sustained turbulence and must be represented by the calculations. Even if their study was focused on the precise determination of the minimal width of the computational domain, an estimate for the streamwise wavelength gave $L_x^+ = 400$–600. This is approximately the length of the near-wall, quasi-streamwise vortical structures, which are significantly shorter than the low-speed streaks they produce, which extend up to thousands of viscous length units, as reported, for example, by Kim and Hussain (1993).

Turbulence Statistics

In this Section, we report a few turbulence statistics. Thanks to the ergodic hypothesis, they are averaged over time and the homogeneous spanwise direction z. Contrary to the standard channel flow, statistics may be computed to depend on the x location over the sinnusoidal distribution of transpiration wave.

Averaged Statistics

In this Section, we report quantities averaged also over the transpiration wavelength. **Figure 5** shows the modification induced in the mean velocity profile by the transpiration with amplitude $A = 0.02U_P$, for two cases with $\alpha_s h = 1.5$ and $\alpha_s h = 4.5$ (case 9 and 19 in **Table 1**), and corresponding to a drag increase and a drag reduction, respectively. As expected from the observation that the mean friction increases in case 9 and decreases in case 19, the two profiles show opposite behavior. Case 9, with longer wavelength, induces an overall larger velocity in the very near-wall region, then a velocity deficit can be observed for $0.05 < y/h < 0.3$. This velocity deficit has to be compensated for in the outer region, since the calculations are carried out at a constant flow rate. On the other hand, case 19 with smaller suction wavelength produces smaller effects (barely discernible on this scale), but in the direction of reducing the slope of the velocity profile at the wall.

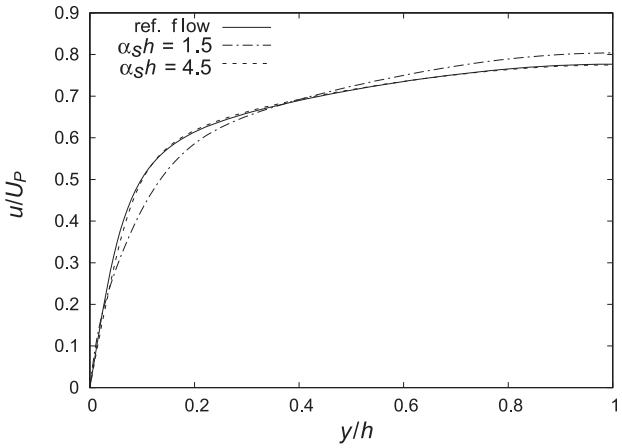

Figure 5. Mean streamwise velocity profile for cases 9 and 19, compared with the reference flow (continuous line).

A better look at the same data can be taken by scaling them with near-wall variables, as shown in **Figure 6**. Each velocity profile is made non-dimensional by means of the friction velocity computed on the basis of the average friction of the corresponding computational case. Case 9 presents the standard characteristics of a turbulent flow over a rough wall, with a drag increase and a consequent downward shift of the logarithmic portion of the velocity profile. Case 19 presents a reduced friction drag, with the consequent upward shift. This is a general feature of drag-reducing flows. There is, however, an important difference with standard flows with drag reduction, which are homogeneous in the streamwise direction. In these

© 2005 CASI

Table 1. Changes in friction coefficient C_f induced by different combinations of A and α_s.

Case	$\alpha_s h$	A/U_p	$10^3 C_f$	%
0	0	0	8.22	0.0
1	0.75	0.08	40.06	387.2
2	0.75	0.04	26.66	224.2
3	0.75	0.02	16.84	104.8
4	0.75	0.01	11.39	38.5
5	0.75	0.005	9.06	10.2
6	0.75	0.002	8.35	1.5
7	1.5	0.08	20.10	144.4
8	1.5	0.04	17.76	115.9
9	1.5	0.02	12.29	49.4
10	1.5	0.01	9.14	11.2
11	1.5	0.005	8.39	2.0
12	1.5	0.002	8.20	–0.3
13	3	0.04	9.24	12.3
14	3	0.02	8.13	–1.1
15	3	0.01	8.09	–1.6
16	4.5	0.08	8.06	–2.0
17	4.5	0.04	7.97	–3.0
18	4.5	0.03	7.86	–4.4
19	4.5	0.02	7.91	–3.8
20	4.5	0.01	8.05	–2.1
21	4.5	0.005	8.15	–1.0
22	6.75	0.08	8.16	–0.7
23	6.75	0.04	8.05	–2.1
24	6.75	0.02	7.99	–2.8
25	6.75	0.01	8.11	–1.3

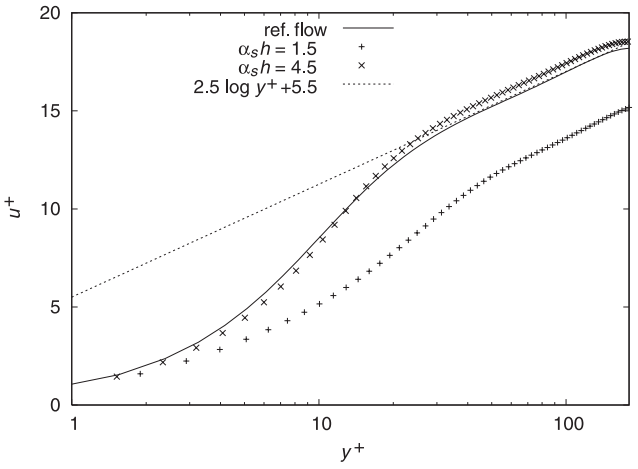

Figure 6. Mean velocity profile plotted in wall units for case 9 and case 19, compared with the reference case (continuous line). Dotted line is the universal law of the wall $u^+ = 2.5 \log y^+ + 5.5$.

cases, the mean velocity profile remains uniformly higher than the reference profile for the standard unmanipulated turbulent flow, see, for example, Quadrio and Sibilla (2000) for drag-reducing flow over an oscillating wall. Here, we can observe the presence of a near-wall region, extending approximately for the extent of the viscous sublayer, where, as a consequence on the local non-equilibrium due to the streamwise variations, the velocity profile with transpiration attains smaller values. We recall, however, that this profile is the result of an average over the entire wavelength.

In **Figure 7,** we report the root-mean-square values of the fluctuations for the longitudinal velocity distribution, averaged over the whole wavelength, as a function of the distance from the wall. The actual friction velocity is used. The results are consistent with the previous observations. In absolute values, case 9 shows significant changes that extend to a significant portion of the channel, but these changes are absorbed by the non-dimensionalization with the actual friction velocity. A generalized increase in the fluctuations in the near-wall region can be observed regardless of the adopted discretization. The peak value is essentially unchanged. Case 19, on the other hand, presents smaller modifications limited to $y^+ < 30$, where the fluctuation level decreases, except for the very near-wall region $y^+ < 4$. The peak position is shifted outwards, suggesting an increase of the viscous sublayer thickness, and the peak value is slightly reduced. The outer layer is unchanged when scaled with the proper friction velocity.

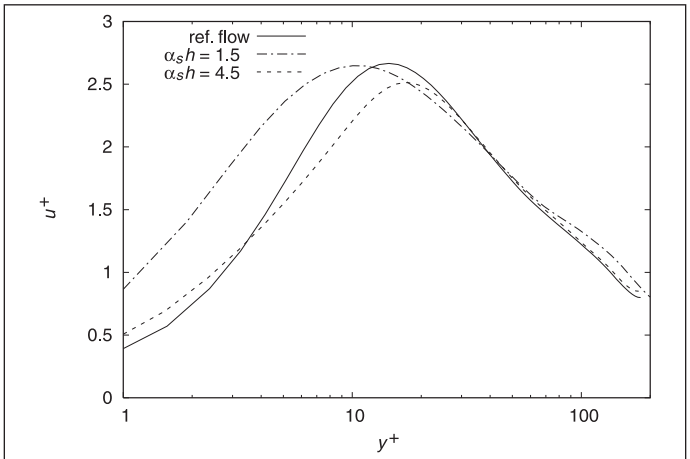

Figure 7. Root-mean-square value of the u velocity fluctuations, averaged over the whole suction distribution: comparison between case 9, case 19, and reference flow.

Turbulence Statistics at Different Positions Along the Wave

In this section we now examine some statistics that are defined to depend on the streamwise position over the transpiration wave.

We show first, in **Figure 8,** the mean velocity profile in the near-wall region for case 9, at four different streamwise positions over a single wavelength. An outer scaling is used, and only the near-wall region is shown. As expected, in the region where the blowing velocity away from the wall is maximum, i.e., $x = 0$, the slope of the mean velocity profile is the lowest. On the other side, where the suction is maximum, the local friction is maximum. The same plot for case 19 (not shown) has a similar qualitative behavior, but the observed differences are much smaller.

© 2005 CASI

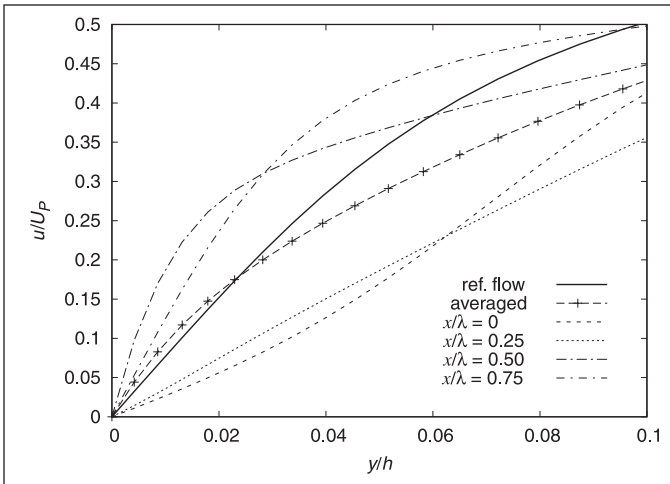

Figure 8. Streamwise mean velocity profile in different positions along the suction distribution: comparison between the wave-averaged profile for case 9 (line with symbols), and the reference flow (thick continuous line).

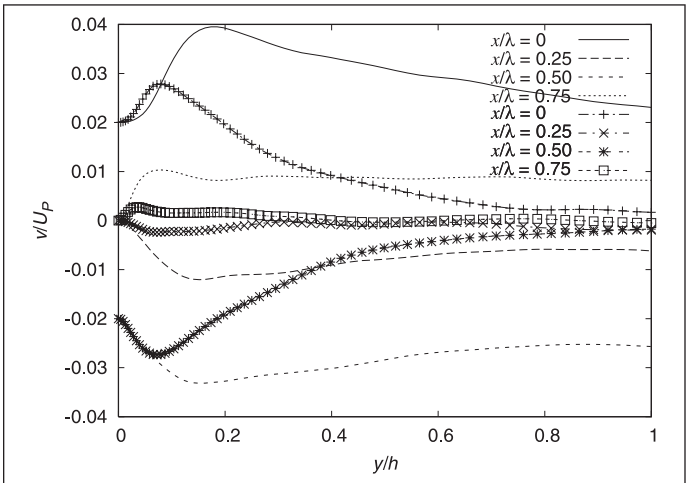

Figure 9. Vertical mean velocity profile in different positions along the suction distribution, case 9 (lines) and case 19 (lines with symbols) at positions $x = 0$, $x = \lambda_s/4$, $x = \lambda_s/2$, and $x = 3\lambda_s/4$.

In **Figure 9**, the mean profile of the wall-normal velocity component at different locations over the suction distribution is reported. In the standard channel flow this profile is identically zero. Profiles for cases 9 and 19 are compared at the same position over the suction wavelength. It can be appreciated how case 19, characterized by a shorter wavelength, has a shorter penetration distance into the boundary layer. The wall values at corresponding positions are obviously the same. A distinctive feature is the peak far from the wall at $x = 0$ that is present in both cases, with different intensity in different positions. At $x = 0$ for case 9 the actual peak is at $y^+ \approx 40$, and its value is almost twice the value of the blowing velocity at the wall.

Conclusions

The effect of a distributed sinusoidal transpiration at the walls of a turbulent channel flow has been examined, by carrying out a number of Direct Numerical Simulations and by systematically changing both the intensity A and the wavelength λ_s of the transpiration. From the preliminary results reported in this paper, a significant effect of the transpiration wavelength can be noticed. For relatively long wavelengths, we find a dramatic increase in the turbulent drag for relatively small values of the maximum velocity at the wall. When the wavelength is decreased below a threshold value, $\lambda_s \approx 2.5h$ or $\lambda^+ \approx 400$, this effect disappears, and an opposite effect takes place: a small but definite reduction of the friction drag is measured.

These results suggest that, contrary to what is generally stated or assumed in most investigations carried out to date for turbulent flows over wavy walls, the wavelength of the waviness may be an important parameter of the flow. In particular we have described a possible link between the value of the wavelength expressed in wall units and a length scale that is typical of the near-wall turbulence cycle.

Acknowledgments

This work has been carried out while M.Q. was visiting the University of Western Ontario, with financial support by SHARCNET (http://www.sharcnet.ca) through their Senior Visiting Fellowship Program. The authors also acknowledge the use of SHARCNET's computational resources and the assistance of SHARCNET's technical support staff.

References

Bechert, D.W., Bruse, M., Hage, W., van der Hoeven, J.G.T., and Hoppe, G. (1997). "Experiments on Drag-Reducing Surfaces and Their Optimization with an Adjustable Geometry". *J. Fluid Mech*. Vol. 338, pp. 59–87.

Berger, T.W., Kim, J., Lee, C., and Lim, J. (2000). "Turbulent Boundary Layer Control Utilizing the Lorentz Force. *Phys. Fluids*, Vol. 12, No. 3, pp. 631–649.

Bewley, T. (2001). "Flow Control: New Challenges for a New Renaissance". *Prog. Aerosp. Sci*. Vol. 37, pp. 21–58.

Bewley, T., Moin, P., and Temam, R. (2001). "DNS-based Predictive Control of Turbulence: An Optimal Benchmark for Feedback Algorithms". *J. Fluid Mech.* Vol. 447, pp. 179–225.

Cabal, A., Szumbarsky, J., and Floryan, J.M. (2002). "Stability of Flow in a Wavy Channel". *J. Fluid Mech*. Vol. 475, pp. 191–212.

Cherukat, P., Na, Y., Hanratty, T.J., and McLaughlin, J.B. (1998). "Direct Numerical Simulation of a Fully Developed Turbulent Flow over a Wavy Wall". *Theor. Comput. Fluid Dyn*. Vol. 11, pp. 109–134.

Choi, H., Moin, P., and Kim, J. (1994). "Active Turbulence Control for Drag Reduction in Wall-Bounded Flows". *J. Fluid Mech*. Vol. 262, pp. 75–110.

De Angelis, V., Lombardi, P., and Banerjee, S. (1997). "Direct Numerical Simulation of Turbulent Flow over a Wavy Wall". *Phys. Fluids*, Vol. 9, pp. 2429–2442.

© 2005 CASI

Du, Y., Symeonidis, V., and Karniadakis, G.E. (2002). "Drag Reduction in Wall-Bounded Turbulence via a Transverse Travelling Wave". *J. Fluid Mech*. No. 457, pp. 1–34.

Floryan, J.M. (1997). "Stability of Wall-Bounded Shear Layers in the Presence of Simulated Distributed Roughness". *J. Fluid Mech.* Vol. 335, pp. 29–55.

Floryan, J.M. (2002). "Centrifugal Instability of Couette Flow over a Wavy Wall". *Phys. Fluids*, Vol. 14, No. 1, pp. 312–322.

Gong, W., Taylor, P.A., and Dörnbrack, A. (1996). "Turbulent Boundary-Layer Flow over Fixed Aerodynamically Rough Two-Dimensional Sinusoidal Waves". *J. Fluid Mech*. Vol. 312, pp. 1–37.

Gschwind, P., Regele, P., and Kottke, V. (1995). "Sinusoidal Wavy Channel with Taylor-Görtler Vortices". *Exp. Therm. Fluid Sci*. Vol. 11, pp. 270–275.

Günther, A., and Rudolph von Rohr, P. (2003). "Large-Scale Structures in a Developed Flow over a Wavy Wall". *J. Fluid Mech*. Vol. 478, pp. 257–285.

Ho, C.-M., and Tai, Y.-C. (1998). "MEMS and Fluid Flow". *Annu. Rev. Fluid Mech.* Vol. 30, pp. 579–612.

Hudson, J.D., Dykhno, L., and Hanratty, T.J. (1996). "Turbulence Production in Flow over a Wavy Wall". *Exp. Fluids*, Vol. 20, pp. 257–265.

Jiménez, J. (2004). "Turbulent Flows over Rough Walls". *Annu. Rev. Fluid Mech.* Vol. 36, pp. 173–196.

Jiménez, J., and Moin, P. (1991). "The Minimal Flow Unit in Near-Wall Turbulence". *J. Fluid Mech*. Vol. 225, pp. 213–240.

Jiménez, J., Uhlmann, M., Pinelli, A., and Kawahara, G. (2001). "Turbulent Shear Flow over Active and Passive Porous Surfaces". *J. Fluid Mech*. Vol. 442, pp. 89–117.

Joshy, S.S., Speyer, J.L., and Kim, J. (1997). "A System Theory Approach to the Feedback Stabilization of Infinitesimal and Finite-Amplitude Perturbations in Plane Poiseuille Flow". *J. Fluid Mech*. Vol. 332, pp. 157–184.

Jung, W.J., Mangiavacchi, N., and Akhavan, R. (1992). "Suppression of Turbulence in Wall-Bounded Flows by High-Frequency Spanwise Oscillations". *Phys. Fluids* A, Vol. 4, No. 8, pp. 1605–1607.

Kim, J., and Hussain, F. (1993). "Propagation Velocity of Perturbations in Turbulent Channel Flow". *Phys. Fluids* A, Vol. 5, No. 3, pp. 695–706.

Kim, J., Moin, P., and Moser, R. (1987). "Turbulence Statistics in Fully Developed Channel Flow at Low Reynolds Number". *J. Fluid Mech.* Vol. 177, pp. 133–166.

Koumoutsakos, P. (1999). "Vorticity Flux Control for a Turbulent Channel Flow". *Phys. Fluids*, Vol. 11, No. 2, pp. 248–250.

Lee, C., Kim, J., and Choi, H. (1998). "Suboptimal Control of Turbulent Channel Flow for Drag Reduction". *J. Fluid Mech*. Vol. 358, pp. 245–258.

Luchini, P., and Quadrio, M. (2002). "Adjoint DNS of Turbulent Channel Flow". In *Proceedings of the 2002 ASME Joint U.S.-European Fluids Engineering Conference*, 14–18 July 2002. Montreal, Quebec. American Society of Mechanical Engineers, New York.

Luchini, P., and Quadrio, M. (2005). "A Low-Cost Parallel Implementation of Direct Numerical Simulation of Wall Turbulence". *J. Comput. Phys.* In press.

Marati, N., Casciola, C.M., and Piva, R. (2004). "Energy Cascade and Spatial Fluxes in Wall Turbulence". *J. Fluid Mech*. Vol. 521, pp. 191–215.

Moin, P., and Mahesh, K. (1998). "Direct Numerical Simulation: A Tool in Turbulence Research". *Annu. Rev. Fluid Mech*. Vol. 30, pp. 539–578.

Phillips, W.R.C., Wu, Z., and Lumley, J.L. (1996). "On the Formation of Longitudinal Vortices in a Turbulent Boundary Layer over Wavy Terrain". *J. Fluid Mech.* Vol. 326, pp. 321–341.

Quadrio, M., and Luchini, P. (2001). "A 4th Order Accurate, Parallel Numerical Method for the Direct Simulation of Turbulence in Cartesian and Cylindrical Geometries". *Proceedings of the XV AIMETA Conference on Theoretical Applied Mechanics* 2001.

Quadrio, M., and Ricco, P. (2004). "Critical Assessment of Turbulent Drag Reduction Through Spanwise Wall Oscillation". *J. Fluid Mech*. Vol. 521, pp. 251–271.

Quadrio, M., and Sibilla, S. (2000). "Numerical Simulation of Turbulent Flow in a Pipe Oscillating Around its Axis". *J. Fluid Mech*. Vol. 424, pp. 217–241.

Robinson, S.K. (1991). "Coherent Motions in the Turbulent Boundary Layer". *Annu. Rev. Fluid Mech*. Vol. 23, pp. 601–639.

© 2005 CASI